Particle Beam and X-Ray Imaging With Thin CsI Scintillating Plates

L. Cosentino and P. Finocchiaro

***Abstract*—At the Laboratori Nazionali del Sud (LNS), Catania, Italy, in the framework of digital radiography and ion beam diagnostics, the use of thin monocrystal scintillating plates made from CsI(Tl) has allowed us to obtain promising results in terms of high sensitivity, compactness, and handiness. In both techniques, a charge-coupled device camera is used to observe the light produced in the crystal when it is crossed by X-rays, in case of radiography, or by charged particles, in case of beam imaging. Spatial resolution has been measured with X-rays as a function of the plate thickness (100 μm to 2 mm), and particular care has been taken in order to perform the imaging of low-intensity radioactive beams ($I_{\rm beam} < 10^5$ pps) that will be produced with the EXCYT facility at LNS.**

***Index Terms*—Radioactive ion beam imaging, X-ray imaging.**

I. Introduction

In THE last few years, the CsI(Tl) scintillator has gained significant popularity because of its considerable light yield and low hygroscopicity. In particular, it allowed us to perform X-ray nondestructive imaging and high-sensitivity beam diagnostics. Within the framework of the Laboratorio Analisi Non Distruttive (LANDIS) [1] at the Laboratori Nazionali del Sud (LNS), the technique for X-ray imaging makes use of thin monocrystal CsI(Tl) plates as sensors. The advantages, as compared to the traditional technique with radiographs, are mainly the possibility of acquiring X-ray pictures in real time and of handling them with a computer. The operating principle consists of irradiating the plate with an X-ray flux that is modulated in intensity by the sample placed in front of it; the scintillation light thus produced in the scintillator gives rise to the radiographic image. This is finally acquired by a PC by means of a charge-coupled device (CCD) camera. The performance of such a kind of system is primarily measured in terms of the modulation transfer function (MTF).

Regarding the development of devices for beam diagnostics, we mainly took into consideration imaging and profiling low-intensity radioactive beams, since in the near future the Exotics with Cyclotron and Tandem (EXCYT) facility at LNS [2] will allow the production of radioactive ion beams. The beam energy will range from 0.2 up to 8 MeV/A; its emittance will be $\varepsilon < 1\pi$ mm·mrad; and its energy spread $\Delta E/E < 10^{-4}$. The facility is based on the isotope separator on-line (ISOL) two accelerators method, in which a stable ion beam is accelerated by a primary accelerator and impinges on a thick target, where it is stopped. The produced radioactive species are continuously extracted, selected in mass, and finally accelerated by a postaccelerator. To have a suitable check of the beam properties (profile, intensity, ion composition, etc.) for tuning, EXCYT needs an efficient beam diagnostics. Unfortunately, the foreseen low beam intensity (well below 10^8 particles/s) does not allow the use of classical devices based on the measurement of the carried charge (wire devices), since the produced currents (<100 pA) would be too low to be efficiently discriminated from the background noise (~10 pA). Therefore, the adopted solution consists of using particle detectors, which, being sensitive to the energy released by the particles, typically have a better sensitivity. Our research and development activities in the past few years have led to the construction of a series of devices based on particle detectors, such as semiconductors and scintillators. CsI(Tl) plates have been successfully used for beam imaging and profiling, distinguishing between applications for stable and radioactive beams. Imaging of stable beams is obtained by means of ions directly hitting the plate surface. The released energy is converted into scintillation light, so that a light spot representing the transversal profile of the beam is produced. A CCD camera watches the light spot, which is directly observable on a monitor and acquired by a PC. For low-energy radioactive beams, we cannot exploit the kinetic energy of ions. Then the light spot is produced by the radiation, emitted by radioisotopes, which crosses the plate. To prevent the beam from directly hitting and thus contaminating the plate, an inert tape is placed in front of it on which the beam implants. Other techniques make use of a photomultiplier tube (PMT) optically coupled with the plate for beam profile reconstruction and identification of ion species.

II. Digital Radiography

In the framework of nondestructive analysis in the LANDIS activity, which includes applications for antique paintings, we have developed a simple technique in order to perform digital radiography. It is based on the scintillation light produced when a scintillator plate is crossed by X-rays. The overall luminosity depends on the energy lost by each X photon and on the intensity (number of photons per second). To explain the formation of the radiographic image, let us suppose we have an X-ray tube that produces a stable X-ray beam. A plate is used as a screen in order to have a rather homogeneous luminosity produced on the surface. When a sample is placed between the tube and the plate, the resulting X-ray intensity is modulated as a function of the sample density. The corresponding luminosity modulation in the scintillating plate gives rise to the radiographic image.

Manuscript received October 13, 2000; revised January 13, 2001 and March 13, 2001.

The authors are with the Laboratori Nazionali del Sud, Istituto Nazionale di Fisica Nucleare, Catania 95123, Italy (e-mail: cosentino@lns.infn.it; finocchiaro@lns.infn.it).

Publisher Item Identifier S 0018-9499(01)06980-5.

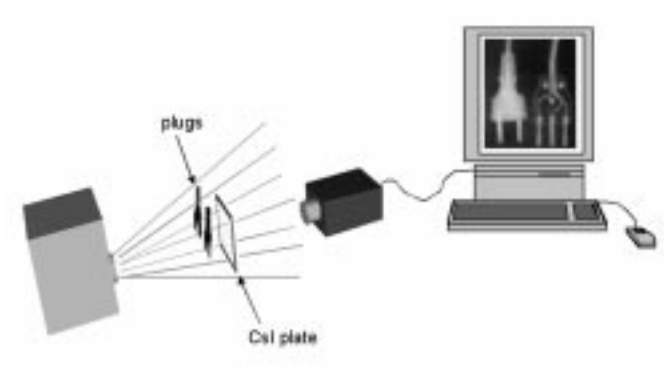

Fig. 1. Scheme of the experimental setup for the radiographic system.

From the analytical point of view, the image can be described by the following exponential relation:

$$I(x, y) = I_0(x, y) \cdot e^{-\mu(x, y) \cdot d(x, y)} \tag{1}$$

where

- (x, y) spatial coordinates on the plate surface;
- I intensity on the plate surface when the sample is put in (I_0 when the sample is removed);
- d, μ respectively, the crossed thickness and the attenuation coefficient of the sample.

In case a digital image is acquired, a suitable software can subtract the systematic noise pixel by pixel, due to the nonuniformity of the impinging radiation and to the CCD background noise, provided that their mean values are stable. The final picture can be represented by the expression

$$e^{-\mu(x, y) \cdot d(x, y)}. \tag{2}$$

A. Experimental Setup and Results

The choice of a monocrystal CsI(Tl) scintillator comes from its high luminous efficiency in order to keep low the statistical fluctuations of the scintillation photons and to reduce the needed dose. The experimental scheme is shown in Fig. 1. The setup consists of a light-tight box, containing the CCD camera (COHU 4910 with 16 mm optics), closed on a side by the blackened scintillating plate. The tube is placed at a suitable distance, so that the plate surface is irradiated rather uniformly. The typical operating voltage is 40 kV; the current is 1 mA.

The performance of this X-ray imaging system has been measured in terms of spatial frequency, with particular care for the spatial resolution. This is affected by contributions coming from the interactions between X-rays and the sample (mainly the Compton scattering) and from the experimental setup, i.e., the CCD pixel size (8.5×8.5 μm^2); the plate thickness, which affects the light spread inside the plate; and the distance between the plate and CCD. To reduce the light spread inside the plate, we use thin plates with thickness from 100 μm to a few millimeters. Plates thinner than 100 μm would be desirable, but they are quite difficult to manufacture.

An analysis in the spatial frequency domain has been carried out by measuring the line spread function (LSF) and calculating its Fourier transform in order to obtain the MTF [3], [4].

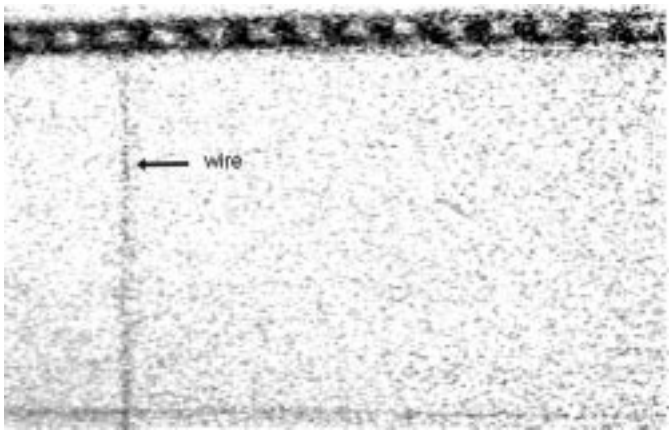

Fig. 2. Radiographic picture of a 100-μm metallic wire. The grid for horizontal calibration is visible in the upper part.

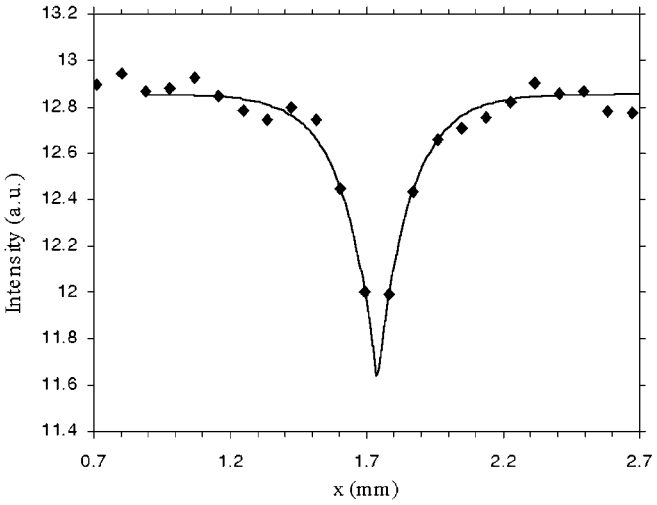

Fig. 3. LSF extracted from the upper picture as the wire transversal profile. Exponential fit is also plotted.

The LSF measurement has been performed by irradiating a thin metallic wire (100 μm diameter) and then extracting the corresponding transversal profile from its X-ray picture. We reported the pixel gray level as a function of x, with x being perpendicular to the wire, and fitted the data with the following exponential function according to [5]:

$$\text{LSF}\,(x) = a + b \cdot \exp - \frac{|x - c|}{d} \tag{3}$$

where

- a and b normalization constants;
- c mean position;
- d related to the width of the curve.

The MTF is obtained by the modulus of the Fourier transform of (3)

$$\text{MTF}\,(f) = \frac{1}{4\pi^2 d^2 f^2} \tag{4}$$

where f is the spatial frequency expressed in line pairs/mm (lp/mm).

Experimental measurements of LSF were carried out for different thickness of the plates: 100 μm, 200 μm, and 2 mm. In

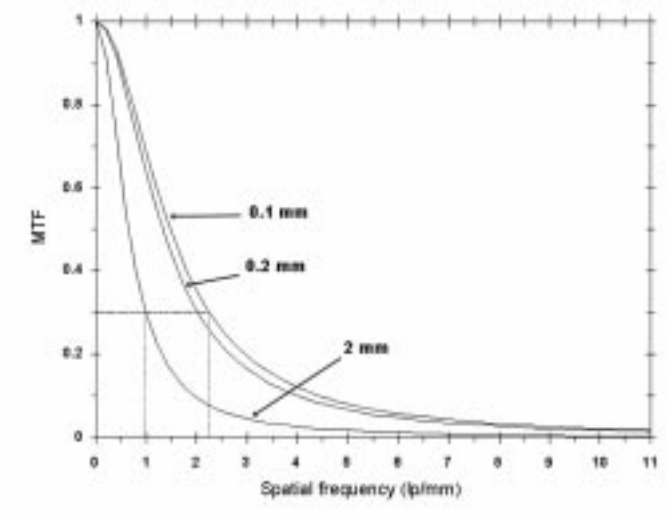

Fig. 4. MTF curves calculated for three CsI(Tl) plates with different thickness. The noise equivalent passband Ne was extracted from the 100-μm and 2-mm curves.

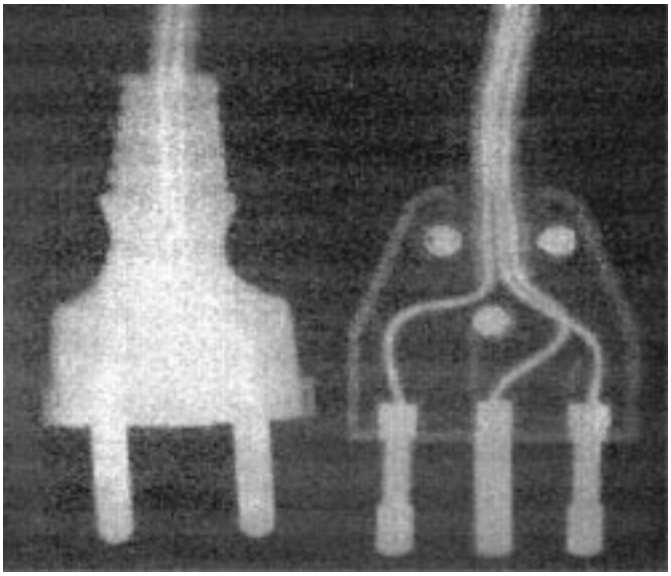

Fig. 5. Radiographic picture acquired with the X-ray camera. The samples are common commercial plugs.

Figs. 2 and 3, an X-ray picture of the wire and its corresponding LSF are shown, respectively; a grid was used in order to perform the x–y calibration of the system.

The MTFs obtained for the three plates are shown in Fig. 4. To compare the different performance of the plates, the noise equivalent passband (Ne), defined as the spatial frequency for 30% of modulation transfer, is extracted from the plots. We measure Ne $= 2.2$ lp/mm for the 100-μm plate and 1 lp/mm for the 2-mm one. It is evident that for a given value of frequency, the MTF becomes lower when increasing the plate thickness. This means that spatial resolution worsens in thicker plates, since the light spread increases. In Fig. 5, we show a radiograph obtained using two ordinary plugs as samples.

III. Beam Diagnostics

Efficient beam diagnostics represents a crucial point for any accelerator facility, since the main requirement of a good beam-tuning is to have an efficient real-time check of the beam properties. This means that along a beam pipe, the diagnostics devices should be able to measure at least the beam current and its transversal profile and to determine the composition in terms of ion species, when possible. These devices can be classified in two main kinds: those sensitive to the charge and those sensitive to the energy of the beam particles. The former include the faraday cups and the wire-based systems; their lower sensitivity threshold is generally around 10^8 particles per second (pps). The latter include the particle detector based systems, whose sensitivity can be made as low as a few pps. Since we are interested in devices suitable for low-intensity beams, we have developed two devices, respectively, for beam imaging and profiling, making use of CsI(Tl) plates.

In particular, we focused on the EXCYT facility, where two accelerators are employed as preaccelerator and booster, respectively. The preaccelerator is a superconducting cyclotron (CS) that accelerates the primary beam with energies up to 80 MeV/A. This beam is transported onto a target-ion source complex, placed on a 250-kV platform. Here, it penetrates and is stopped inside a thick graphite target, where many radioactive nuclear species are produced. These products are then extracted, ionized (charge state -1), and selected in mass by a high-resolution isobaric separator ($\Delta M/M < 1/20\,000$), installed ahead of the booster (a 15-MV Van De Graff tandem).

A. High- and Low-Energy Beam Profiler

Regarding the beam profiling, our solution is a scintillator-based beam sensor (SBBS), consisting of a $1 \times 1 \times 0.5$ cm^3 CsI(Tl) crystal arranged behind a thick graphite screen with a 0.5-mm slit [6], Fig. 6.

A compact photomultiplier is optically coupled to the scintillator, so that the whole structure can be moved to scan the beam with the slit. By plotting the PMT output current as a function of the position, the transversal profile is carried out. Experimental tests have shown a high sensitivity, as this device is able to reconstruct beam profiles with intensities below 10^4 pps. For $I_{\mathrm{beam}} < 10^5$ pps, SBBS is also able to count the single particles, by means of a discriminator and a scaler, thus allowing the self-calibration (light versus counts). We have also proved that SBBS can operate at very low energy, easily sensing a 1-pA beam of ^{12}C at 50 keV in current mode. Unfortunately, at such a low energy, single particles cannot be counted, since the scintillation light produced by each particle is not enough to form a pulse detectable by the discriminator, and therefore in such a case self-calibration is not feasible.

Taking into account the properties of the EXCYT beams at LNS, the foreseen transversal beam size after the acceleration is on the order of a few millimeters, and a space resolution of about 0.5 mm, as achieved with SBBS sensors, seems reasonable.

B. Low-Energy Beam Imager/Identifier

A difficult task is sensing, imaging, and identifying the beam before its acceleration: the low energy and intensity of the ra-

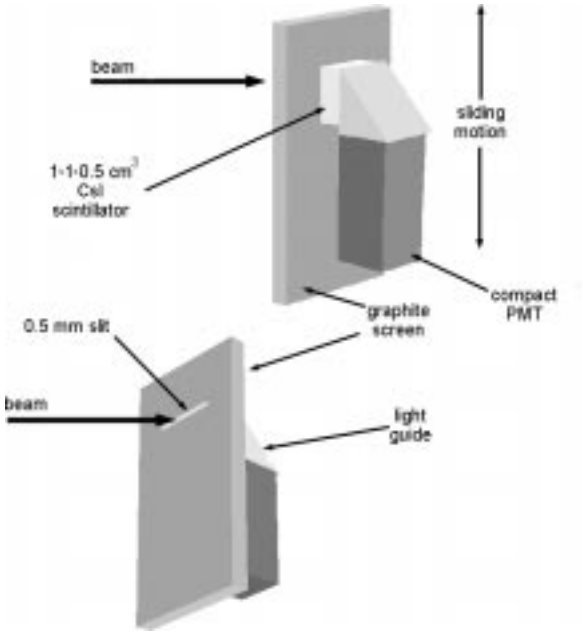

(a)

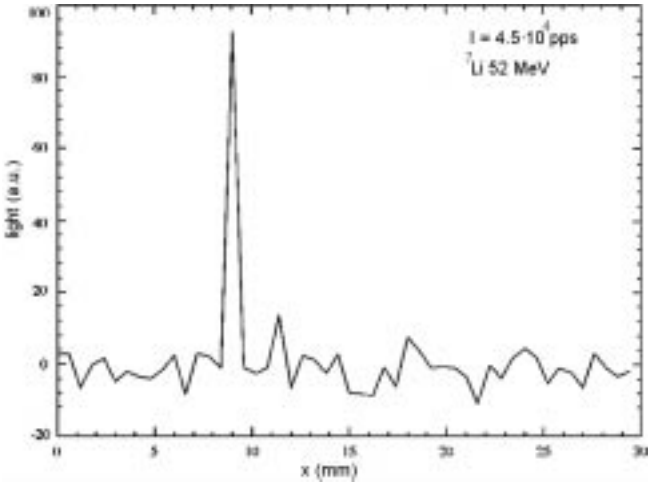

(b)

Fig. 6. (a) Sketch of the SBBS device and (b) example of acquired beam profile.

dioactive beam, as it emerges from the mass separator, will still be several millimeters wide. However, the space separation between its different isobaric components, which depends on their mass excess, can range from a few millimeters in the most favorable cases (light species) to a few hundred micrometers in the worst ones (heavy species).

Making use of CsI(Tl) plates, we have developed a device for the beam imaging and identification, to be installed on the preacceleration stage along the beam pipe, between the target ion-source complex and the tandem accelerator [7]. This device, the low-energy beam imager/identifier (LEBI), basically consists of a CsI(Tl) plate, 1 or 2 mm thick, and of a 6-μm mylar tape arranged in front of the plate at a distance of 0.5 mm (Fig. 7). When the radioactive beam hits the tape, it gets implanted because of its low energy (up to 300 keV). After the decay, roughly half of the emitted β- and γ-rays cross the plate. This radiation is emitted isotropically, and since a large fraction of the solid angle covered by the plate is close to the emission point, the sum of the contributions due to each beam particle gives rise to a light spot, whose diameter is larger than the transversal size of the beam. The spot intensity is related to the beam intensity, to the activity of the implanted nuclei, and to the type and energy of the radiation produced by the decay.

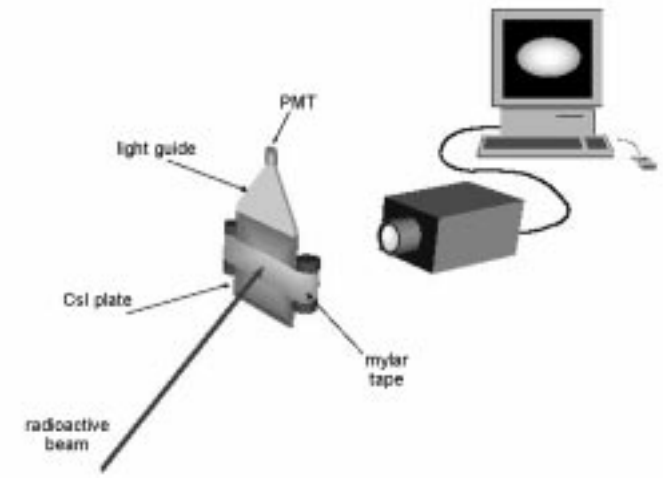

Fig. 7. Sketch of the LEBI device for low-energy beam imaging and identification.

The spatial resolution of LEBI is rather modest. In fact, if a hypothetical point-like source is placed in front of the plate, the radiation will cross the plate in all directions (the plate covers a solid angle of about 2π sr), thus producing a light spot with a halo around it. The full-width half-maximum (FWHM) of the spot profile represents the spatial resolution of the system, which is on the order of the plate thickness—in our case, between 1 and 2 mm.

Since no radioactive beam is available so far from EXCYT, an experimental test has been performed by using an uncollimated ^{90}Sr beta source, with 3-mm diameter and 31-MBq activity (the source decay chain produces two beta particles, with endpoint energy of 546.2 and 2280.1 keV, respectively). It was placed in front of the 2-mm-thick CsI plate at a distance of 1 mm from it. The well-visible light spot obtained with this plate is shown in Fig. 8. Its transversal profile has been fitted with a Gaussian curve with FWHM ≈ 3.5 mm. Another test has been performed, still with the 2-mm plate, by using a 1-mm collimator that reduces the beta-ray intensity down to 10^3 pps. The detected light spot has a FWHM ≈ 1.8 mm; by using the rule of the sum of the squares, we calculated a spatial resolution of $\Delta x \approx 1.5$ mm for this device.

The LEBI prototype we have built is made of a spherical vacuum chamber containing the plate-tape setup. The tape is rolled up in two spools and can be slid on, whenever it becomes contaminated, by means of a dc motor (Minimotor 3557K012). An external high-sensitivity CCD camera (Watec WAT–902H, sensitivity of $3{\cdot}10^{-4}$ lux) watches the plate in order to acquire the images. A pneumatic cylinder allows one to insert and remove the plate-tape setup from the beam line via remote control.

The device sensitivity is strongly bound to the radioactive nuclear species under consideration; however, we have proved

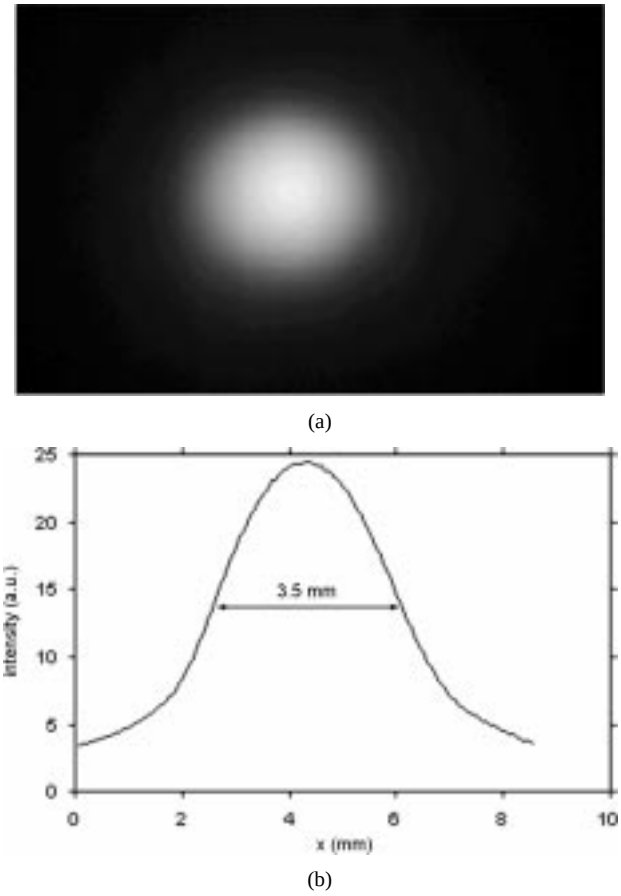

Fig. 8. (Top) Sample picture taken with LEBI using a circular 10^7Bq ^{90}Sr source. (Bottom) Integral profile of the light spot; the FWHM is 3.5 mm. The diameter of the source is 3 mm.

that with a 1-mm collimated point-like ^{90}Sr source, the system is sensitive at least down to 10^3 pps. To have specific information about sensitivity, each nuclear species has to be considered as a particular case.

To study how LEBI should display the beams transported along the beam pipe of EXCYT, we developed a Monte Carlo simulation code, based on the energy loss of beta-rays inside the crystal. It is capable of simulating the shape of the light spot produced by the radiation crossing the plate. As an example where a realistic beam is simulated, we assumed production of a ^{18}F beam that contains ^{18}N as a contaminant. Using beam transport calculations, we derived the transverse distribution of the two ion species after the mass separator; the foreseen separation between the centroids is 4.8 mm. Then we used these results as input to the LEBI simulation code, whose output is reported in Fig. 9. The spatial separation between the main beam and the contaminant is evident. The predominance of the contribution due to ^{18}N ions depends on the value of its decay constant ($\lambda_{18N} = 1.11\ \mathrm{s}^{-1}$), which is much larger than ^{18}F ($\lambda_{18F} = 1.05 \cdot 10^{-4}\ \mathrm{s}^{-1}$).

To obtain as much information as possible to identify the beam, a small photomultiplier (Hamamatsu R7400U) used in pulse-counting mode is optically coupled to a plate side by means of a specially suited light guide. It may be helpful for the identification of the implanted nuclei, allowing one to reconstruct its decay curve by measuring the counting rate and

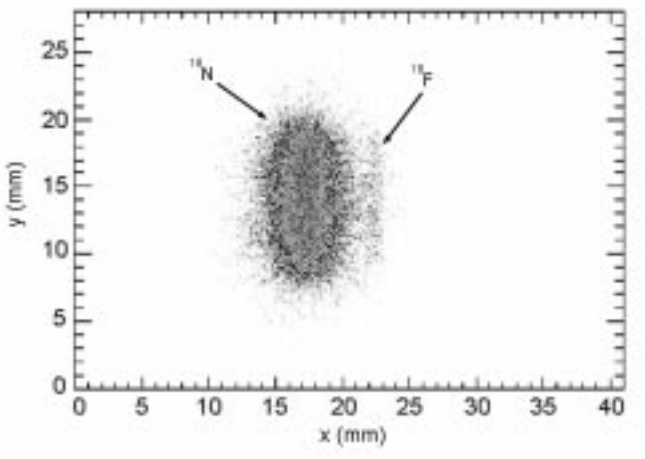

Fig. 9. Simulated response of LEBI for a ^{18}F beam. Main contaminant ^{18}N contributes very much to the image because of its higher decay constant.

then to evaluate the decay constant λ. A more accurate analysis can be carried out by using two germanium detectors, which are foreseen to be installed sideways, and that may allow one to identify the implanted nuclides by acquiring their gamma spectra.

IV. Conclusion

CsI(Tl) was known to be a powerful scintillator, being able to satisfy a wide range of requirements. We have shown that in the form of thin monocrystal plates, it can be fruitfully exploited for imaging, achieving good quality and sensitivity at low cost with a simple setup. Both applications, beam diagnostics and X-ray imaging, look very promising in view of future developments.

Acknowledgment

The authors would like to thank G. Pappalardo and P. Romano for providing the X-ray tube. They would also like to acknowledge the help given by A. Vinciguerra and S. Cappello during their work for the diploma thesis.

References

[1] G. Pappalardo and P. Romano, "Feasibility study of a portable PIXE system using ^{2}10Po alpha source (1996)," *Nucl. Instrum. Meth.*, vol. B109, p. 214, 1996.

[2] G. Ciavola, L. Calabretta, G. Cuttone, G. Di Bartolo, P. Finocchiaro, and S. Gammino, *et al.*, "The ISOL exotic beam facility at LNS: The EXCYT project," *Nucl. Instrum. Meth.*, vol. B126, pp. 258–261, 1997.

[3] H. Fujita, D. Tsai, T. Itoh, K. Doi, J. Morishita, and K. Ueda, *et al.*, "A simple method for determining the modulation transfer function in digital radiography," *IEEE Trans. Med. Imag.*, vol. 11, no. 1, pp. 34–39, 1992.

[4] P. Pavan, G. Zanella, R. Zannoni, and A. Marigo, "Spatial resolution in X-ray imaging with scintillating glass optical fiber plates," *Nucl. Instrum. Meth.*, vol. A327, pp. 600–604, 1993.

[5] V. Kaftandjian, "A comparison of the ball, wire, edge and bar/space pattern techniques for modulation transfer function measurements of linear X-ray detectors," *J. X-Ray Sci. Tech.*, vol. 6, p. 205, 1996.

[6] P. Finocchiaro, G. Ciavola, L. Cosentino, M. Gu, G. Raia, and A. Rovelli, "A self calibrating ion beam profiler based on a CsI scintillator," *Nucl. Instrum. Meth.*, vol. A437, pp. 552–556, 1999.

[7] S. Cappello, L. Cosentino, and P. Finocchiaro, "Off-line testing of beam diagnostics devices for characterization of low-intensity radioactive beams," *Nucl. Instrum. Meth.*, to be published.